

INVESTIGATION OF MECHANICAL PROPERTIES OF PLASTER REINFORCED WITH PA MICROFIBER.

F. Parres¹, J.E. Crespo¹, A. Nadal¹, S. Sánchez¹, M. Selles¹

¹ Universitat Politècnica de València, Plaza Ferrándiz y Carbonell, 1 03801 Alcoy
(Alicante) ESPAÑA, fraparga@dimmm.upv.es

Keywords: plaster, fibers, polyamide, mechanical properties, recycled

Abstract: Polyamide fibers have been frequently used as a ceramic and polymer reinforcement, the main advantage of using fiber is to prevent a catastrophic failure of the ceramic material in two pieces. The compression and bending test show differences between samples prepared with different percentages of fiber.

1. INTRODUCTION

In recent years, the re-use of waste materials has become extremely important for two main reasons: economic and environmental. With the first of these, the recovery of material often means a reduction in manufacturing costs of certain products which enables them to compete with virgin products. However, it is the second reason, the environmental impact factor, which is assuming greater importance nowadays. Over the last decade many governments have imposed legislation to deal with this problem. In the case of thermoplastics, recovery processes are generally easy and the simple use of heating allows to get new products with similar characteristics. On the other hand the recovery of other materials such as tires is more complicated as new tires can not be manufactured by recycling old ones. One of the solutions adopted has been the use of recycled tires in other applications such as acoustic insulation, flooring for children's parks and other products obtained from shredded tires. In the tire recovery process several types of fibers are also obtained, including fibers incorporated in the tires for reinforcement. The characterisation and identification of these materials were done using differential scanning calorimetry (DSC). This technique has been used by other authors for the analysis of several polymers [1,2].

Fibers, in general, have been used by several authors in order to improve mechanical properties of fragile materials. In ceramic materials, fiber helps prevent the progression of crack from its origin and also avoid the piece breaking completely in two. Plaster has been traditionally used in glass fiber as reinforcing agent. The aim of this research has been the use of fibers from shredded tires using it in plaster reinforcement.

2. EXPERIMENTAL

2.1. Materials.

Two types of fiber were used: virgin fibers from different sources (the Polyamide 6 and Polyamide 6.6 were supplied by Industrias Químicas Textiles, S.A., Andoain (Guipuzcoa) – Spain); and fibers derived from the tire shredding process, were supplied by Industrias del Neumatico, S.A., Aspe (Alicante) - Spain.

Tires arrive at the recovery plant(,) where, after a first crushing process, are reduced to sizes of about 100mm, then reduced to sizes of about 20 mm by the same process, and finally reduced to small sizes (7 – 0.2 mm) by shredding. The number of stages of crushing

and shredding depend on the desired grain size. We only use crushing in the case of big sizes (100 – 20 mm). In order to obtain grain sizes between (7 – 0.2 mm) we combine crushing and shredding. Steel fibers are separated using electromagnets. The separation of the textile fibers always takes place by aspiration on the sieve which is defined by the desired grain size and by the processes that combine crushing and milling. There are usually two stages of crushing, one reducing the whole tire to 100 mm pieces, and the second reducing this down to 20 mm pieces. The shredding stages vary between one and three based on the desired gain size (7 – 0.2 mm). Crushing and shredding takes place at room temperature and cryogenic processes are not used.

Plaster prepared by hydration with a water ratio of 0.8 is the material used in this research. A series of prismatic test pieces of 160 x 40 x 40 mm (flexural test) and 40 x 40 x 40 mm (compression test) were produced, following RY-85, and each series is formed by three test pieces. The test were performed on the samples after 28 days according to the specifications established in general conditions that are standard for reception of plaster and gypsum in work under construction [3].

2.2. DSC analyses.

Calorimetric analysis was carried out using DSC Mettler-Toledo 821 equipment (Mettler-Toledo, Schwerzenbach, Switzerland). Weight samples between 6 and 7 mg were used. A first heating (30 – 150°C at 10°C min⁻¹) was completed, followed by a cooling process (150 – 30°C at 10°C min⁻¹) to eliminate the thermal history, and was finished with a second heating (30°C at 350°C at 10°C min⁻¹). The tests were performed in a nitrogen environment (flow rate 50 mL min⁻¹).

2.3. Scanning electron microscopy (SEM) measurements.

Fibers and microfibers were analyzed by Scanning Electron Microscopy with a HITACHI S-3000N Scanning Electronic Microscope (Hitachi Ltd. Japan). Image acquisition was taken after gold sputter coating under vacuum on the surface of the samples.

2.4. Mechanical properties measurements.

The mechanical properties of the samples were evaluated using an ELIB 30 electromechanical universal testing machine by Ibertest (S.A.E. Ibertest, Madrid, Spain), with two load cells (5 and 50 kN) to determine the flexion resistance and compression strength of the test pieces. Different concentrations of polyamide fibers (1, 2, and 4 wt %) were first dispersed in water, and then the plaster powder was poured and mixed to obtain the blends.

3. RESULTS AND DISCUSSION

3.1. Morphological study.

A good performance of the compound materials is mainly based on the fibers morphology that was used: length, diameter, surface finish, etc. In this case, it was the mechanical shredding process that determined the final morphology of the fiber. After this process, two main types of fiber can be identified: fiber and microfiber. In the first case, the fibers maintain their original form (cord) and still show some particles of shredded tire

stuck to their surface, while the microfibrils are a consequence of the different stages in the shredding process that break up or unravel the original fibers (Figure 1).

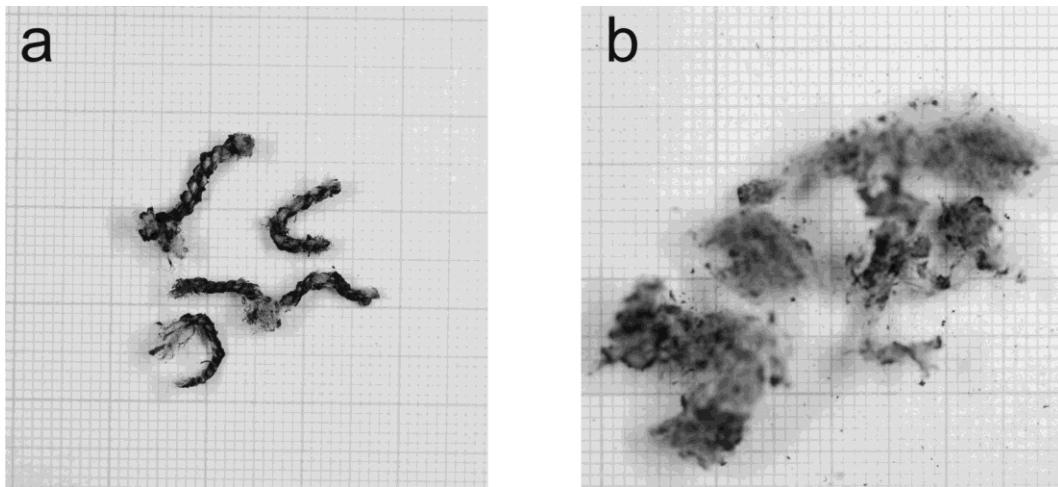


Figure 1. Images of different types of fibre and microfibre after the shredding process. A - fibre, B – microfibre.

Scanning electronic microscopy allows us to observe in more detail the fiber and microfibril morphology. Figure 2-a show us the arrangement of the several microfibrils that make up the fiber (cord) with some tire particles stuck to the surface; nevertheless, the microfibril images allow us to observe the lack of tire particles stuck on their surface (Figure 2-b).

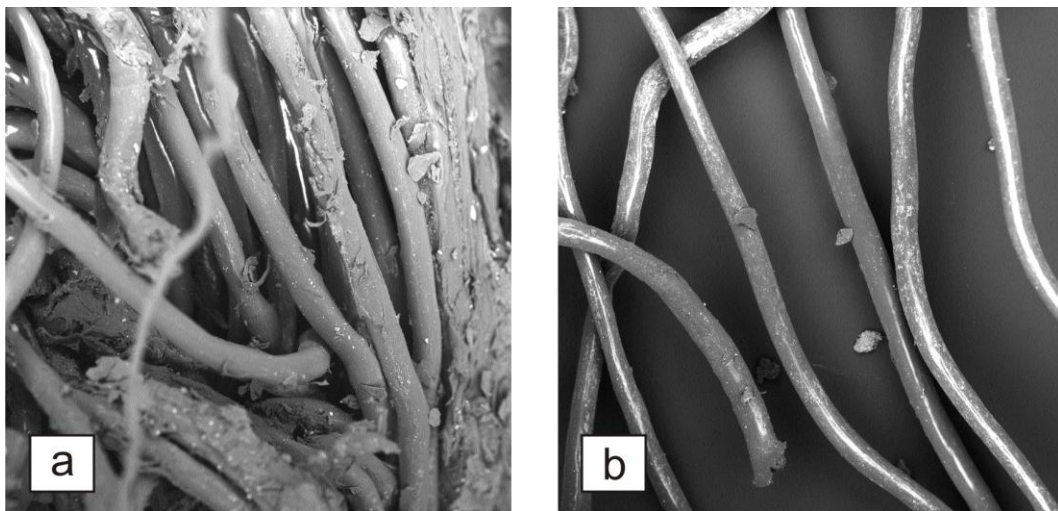


Figure 2. SEM micrograph of fibres (a) and microfibrils (b) (x500).

The manual division of 100 grams of fiber in both fragments shows the existence of a high proportion of microfibril (84%) to fiber (16%).

The statistical study carried out on 20 microfibrils shows a variable length (2 – 8 mm) where the arithmetic mean is around 5 mm. Their diameters are more homogenous and the mean is $29.67 \pm 2.3 \mu\text{m}$ (Figure. 3).

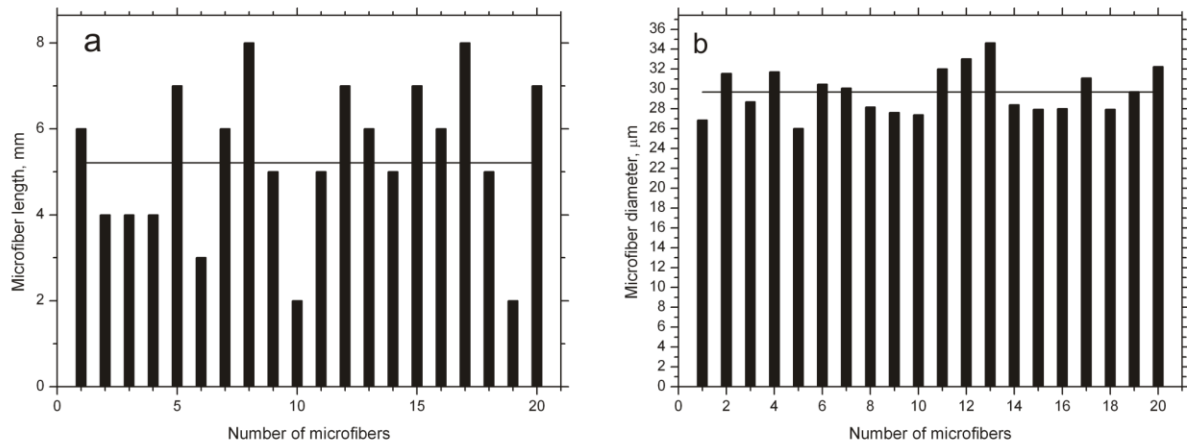


Figure 3. Statistical study of microfibre morphology obtained from shredded tire about 20 ud..

In the same way, the fiber morphology was analyzed. In this case, the study made with 100 fibers showed a variation in length, the shortest being 6 mm long and the longest 26 mm, although the diameter is always around 1 mm. (Figure 4).

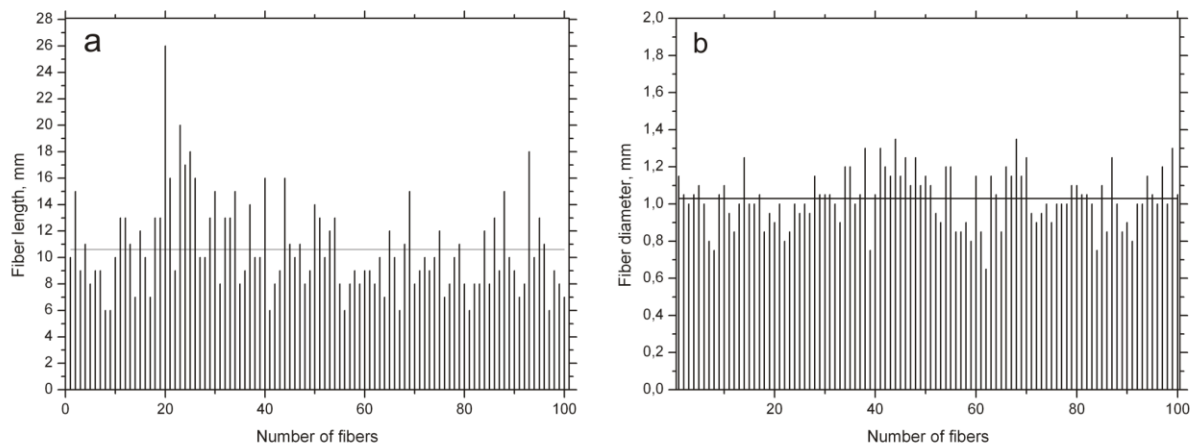


Figure 4. Statistical study of the fibre morphology obtained from shredded tire about 100 ud.

All measurements were made by hand extending fiber and measuring with a rule of accuracy 0.5 mm, except the diameter of the microfiber, which they were obtained by the measurement on the images obtained in scanning electron microscopy. The statistical distribution follows a normal evolution where nearly 98% of fibers are less than 20 mm long, and most of them are between 8 and 10 mm long (Figure 5).

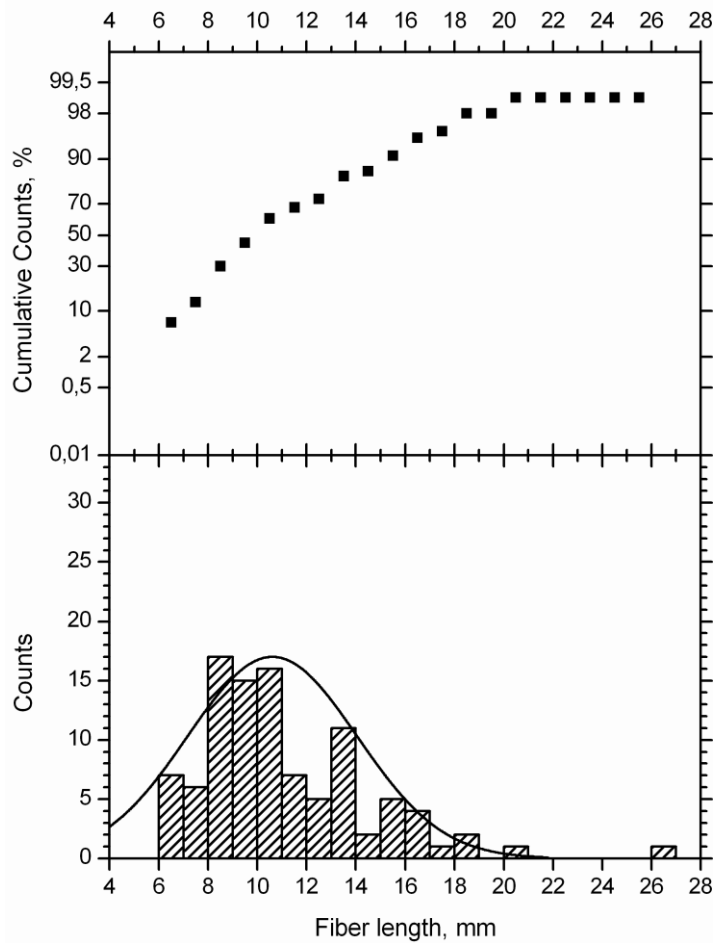


Figure 5. Statistical data on polyamide fibres obtained from shredded tires.

3.2. Thermal analysis, DSC results.

The fibers obtained from the recovery process come from the tire's internal reinforcements incorporated to improve the characteristics of the tire. Over time many fibers of natural origin have been used as reinforcement (cotton or rayon) and synthetic origin (polyamide 6 or polyamide 6.6). Currently, most fibers used are of synthetic origin [4-6].

Differential scanning calorimetry (DSC) has been used by different authors for the identification of materials [7], especially when dealing with polymer materials. This identification is based on localising the different thermal transitions shown by polymers. This technique has also been used to find the initiation of degradation in fibers of natural origin [8].

The identification of polymers using this technique is much more straightforward if control references are used for comparison with the samples being analysed. In this work, calorimetric studies were carried out on two types of fiber: polyamide 6 and polyamide 6.6. These two types will be used as references.

The calorimetric curves show differences between the reference fibers which show endothermic peaks at different temperatures. Polyamides 6 and 6.6 show endothermic peaks corresponding to the melt point of spherulites at about 220 and 260°C respectively (Figure 6) [9].

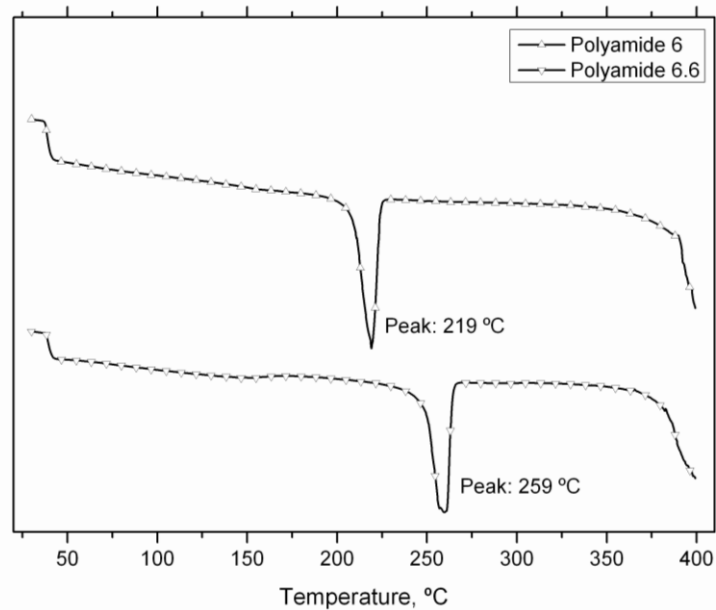


Figure 6. Calorimetric curve of the reference fibres (polyamide 6 and polyamide 6.6).

The low point of the endothermic peak indicates the melt temperature and can be used to identify the fibres obtained from shredded tires. Table 1 shows the melt temperature values of the fibres used as references.

The calorimetric curves of fibres and microfibers are similar. The fibres and the microfibers show two peaks of differing intensity, approximately at 220°C and 260°C. These results show that the fibres used for reinforcement in tires are polyamide 6 and 6.6 (Fig. 7).

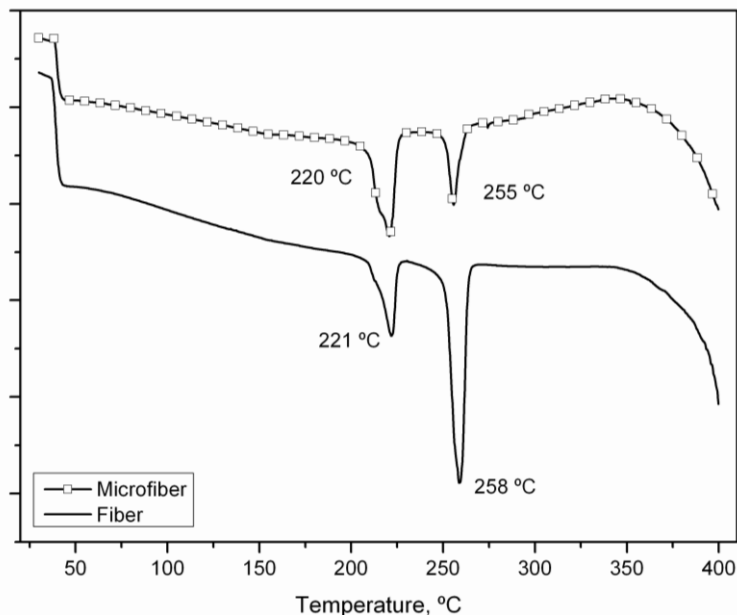


Figure 7. Calorimetric curve of the different tire fibres.

3.3. Mechanical properties

Obviously before analyzing the influence on the plaster matrix, the plaster without fiber has to be characterized.

A typical 3 point stress – strain curve depicted in Fig. 8-a emphasizes the linear elastic performance up to failure, as a result of lineal advance of the crack. Compression

tests show a similar performance. Although, in this case, the test rupture is different, since compression tensions cause the appearance of several cracks that advance at an angle depending on the direction of the force applied depending on the compression load applied and the sliding between the compression plates and the sample to be tested, and so they cause material failure by numerous fractures (Fig. 8-b).

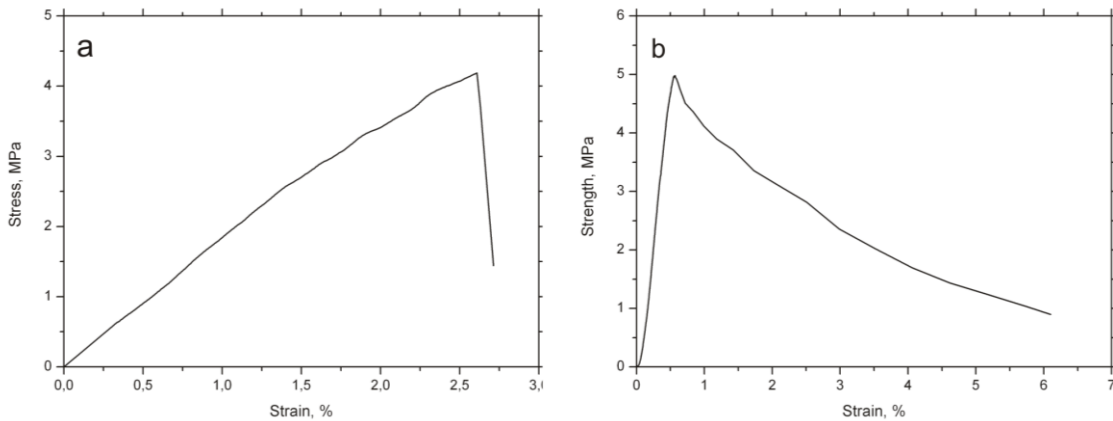


Figure 8. Flexural (a) and compression (b) stress – strain curve typical to the neat plaster.

Table number 2 show the values obtained from the mechanical characterization of the plaster without fiber, which will be used as reference values throughout all the research. The addition of fibers in the plaster causes important differences as far as its mechanical performance under different load stages (flexural and compression) is concerned. The flexure test with a lack of fiber is characterized by a lineal performance until the maximum flexure value (σ_r); once this value has been reached, the rupture of piece is completed and the flexure decreases sharply until zero.

Nevertheless, the existence of fiber causes variations in the rupture process, because once the maximum flexure value has been reached, it decreases sharply until the fiber starts to act and the tension (σ_s) is stabilized by the interaction of the fiber with the matrix phase (plaster) (Fig. 9).

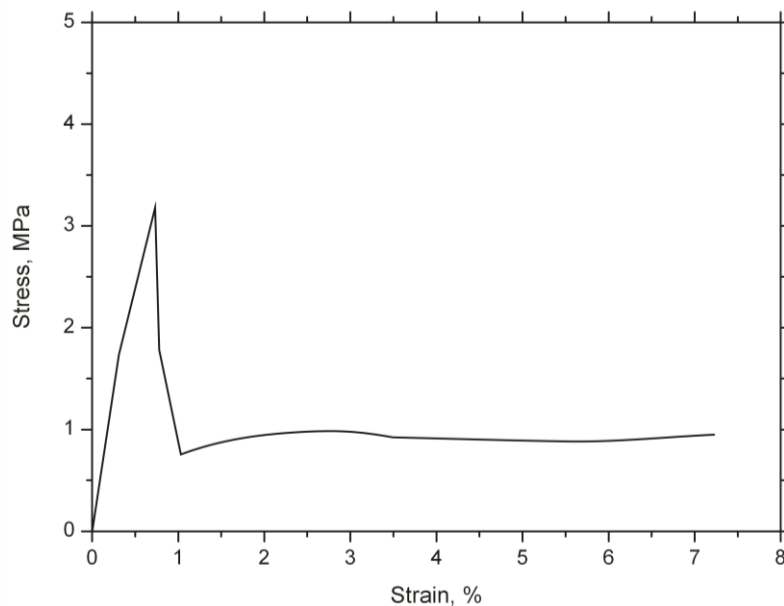


Figure 9. Stress – Strain curve typical to fibre reinforced plaster.

The connection between σ_r and σ_s is known as fiber efficiency factor (FEF) and its value is between 0 and 1, being the highest values indicative of the early performance of the fiber.

$$FEF = \frac{\sigma_s}{\sigma_r} \quad (1)$$

The performance of plaster with fiber is very different depending on the type of effort applied. In the case of the test failure, the addition of fiber causes a sharp decrease in the flexural strength until reaching a loss of 50% for a fiber contents of 4% (Fig. 10-a). Nevertheless, the addition of fiber in plaster causes a different effect on properties obtained after the compression test. In this case, the value evolution shows a slight decrease which represents a loss of only 12% (Fig. 10-b).

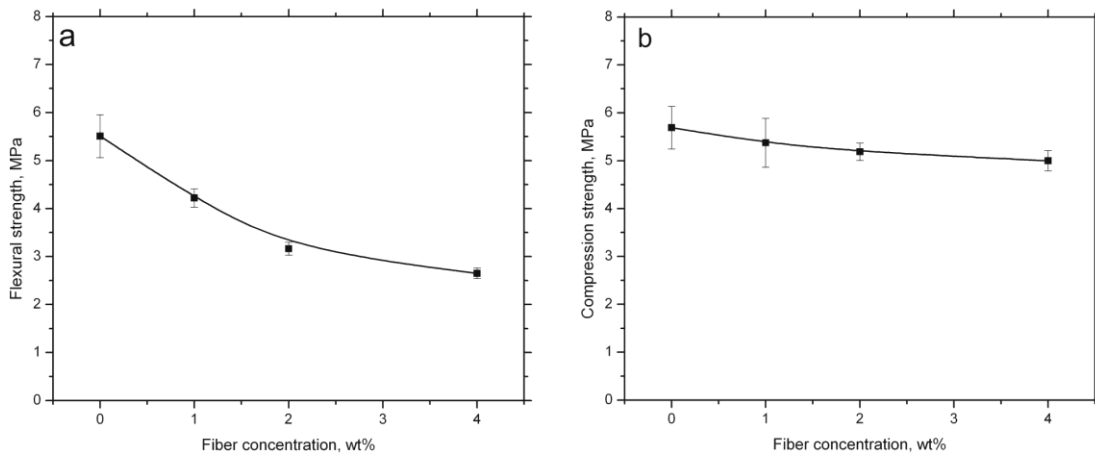


Figure 10. Evolutions of the flexural strength and compression strength of plaster reinforced with PA recycled fibres.

The major benefit of the presence of fibers is to avoid a catastrophic failure of the material in two pieces. In this case, and as has been repeated in other research, the fiber efficiency factor (FEF) value increases with the fiber percentage, and reaches a value of 0.5 for contents of 4% of fiber [10-12] (Fig. 11).

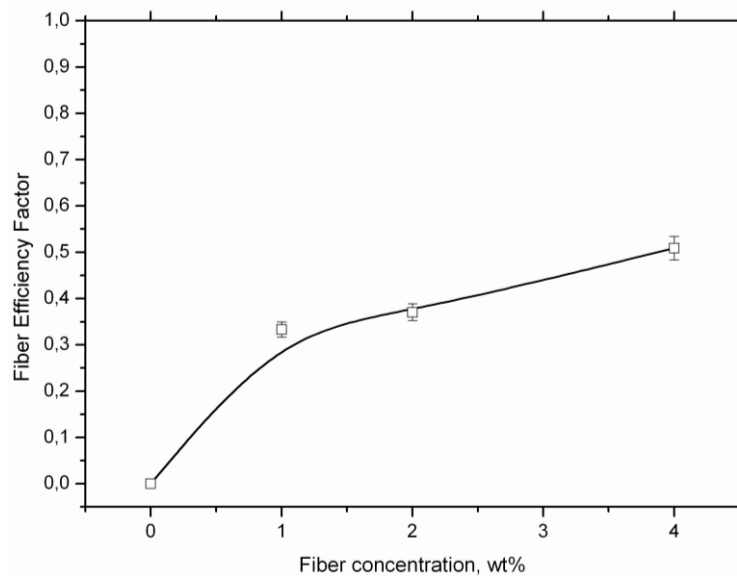


Figure 11. Evolution of the fibre efficiency factor of plaster reinforced with PA recycled fibres.

Given that microfiber is 86% of the total weight of fiber and that fibers smaller than 20 mm represent the biggest percentage (98%) of the fiber obtained after the tire's recovery process, the mixture of plaster with separate fiber, plaster with microfiber (1, 2, and 4 wt%) and plaster with fiber less than 20 mm (1, 2, and 4 wt%) is considered.

In both cases, results show a very similar evolution in flexural strength to that of compression strength, where the increase of the fiber percentage causes a decrease of the flexural strength while the compression strength values remain practically constant (Fig. 12).

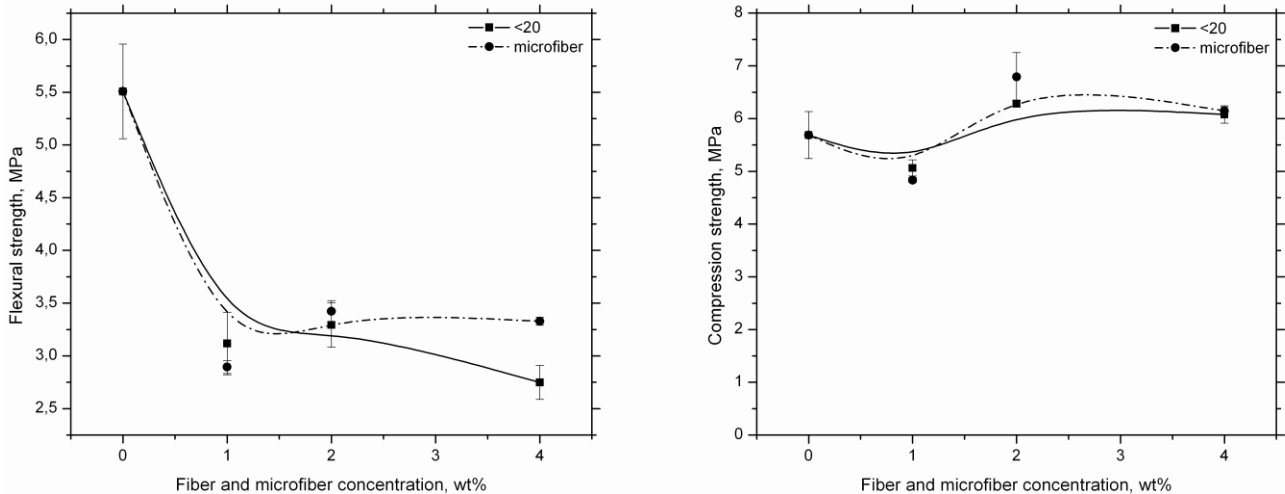


Figure 12. Evolution of the flexural and compression strength of plaster reinforced with PA microfibres and fibres <20 mm.

Nevertheless, the fiber efficiency factor values show some important differences. The plaster mixtures with microfiber show higher values than the ones with fiber. Results show also more efficiency in microfiber, since for low percentages of this (1%), FEF show positive values (0.25). But, with the same percentage, the fiber isn't able to act and its FEF is zero (Fig. 13). This effect is due to a greater level of dispersion of the microfiber in the plaster matrix.

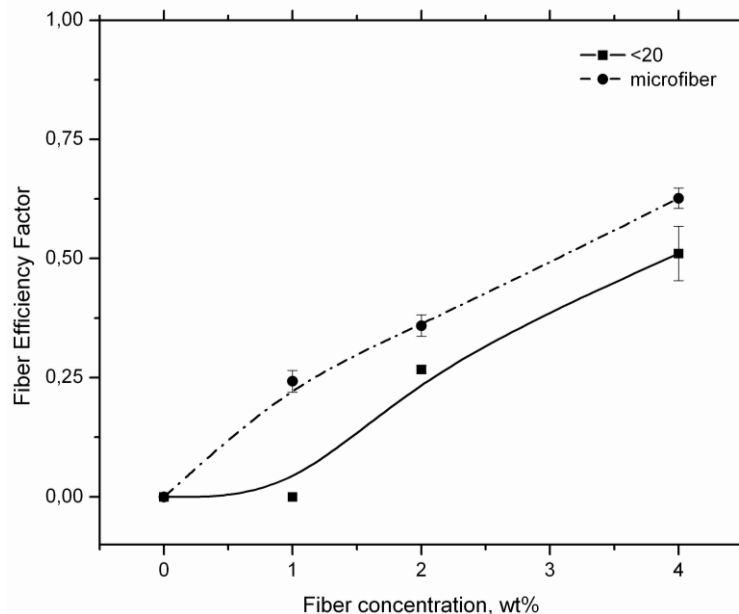


Figure 13. Evolution of the fibre efficiency factor of PA microfibres and fibres (<20mm).

4. CONCLUSION

The final morphology of fibers and microfibers is defined by the tire mechanical shredding process. This process reduces the tire size until most fibers become microfibers. Fiber identification is made by thermal analysis techniques and shows us the presence of two types of polyamide, polyamide 6 and polyamide 6.6.

As far as mechanical performance is concerned, the different plaster mixtures show a tendency very similar to the result observed by other authors with fibers of a different nature, that is to say that flexural strength is substantially reduced with the addition of fibers while compression strength suffers from a light decrease.

The surface morphology of the fiber is one of the key factors in the mechanical properties of composite materials. In this case, the surfaces of the fiber and the microfiber are very different. Initially, the fiber has the highest surface roughness microfiber because it maintains its original form (cord), but the presence of a certain amount of tire rubber adhered to its surface causes a loss of adhesion to the matrix of plaster. For this reason the results for both cases are very similar except for the efficiency factor values are higher in fiber than the microfiber due to its greater dispersion.

Finally, the difficult process of separating the fibers into two parts (fiber and microfiber) performed in our case by hand, can be an impediment for the economic reuse of this waste. The direct use of the fiber without a separation would be a feasible process.

5. ACKNOWLEDGEMENTS

The authors thank the Generalitat Valenciana Ref: GV/2010/017 by the funding received for the development of this research through Projects Emerging Research Group 2010.

6. References

1. HP, Brack; D, Ruegg; H, Buhner; M, Slaski; S, Alkan; GG, Scherer. Differential scanning calorimetry and thermogravimetric analysis investigation of the thermal properties and degradation of some radiation-grafted films and membranes. *J. Polym. Sci. Pt. B-Polym. Phys.* 2004;42:2612-2624.
2. D, Garcia; R, Balart; JE, Crespo; J, Lopez. Mechanical properties of recycled PVC blends with styrenic polymers. *J. Appl. Polym. Sci.* 2006;101:2464-2471.
3. M, del Rio Merino; P, Comino. Disperebility degree influence of glass fiber E in the machanical behaviour and workability of plaster. *Mater Construcc* 2001;51:261.
4. HH, Gillman; R, Thoman. Behavior of Rayon Tire Cord During Latex Dipping. *J Ind Eng Chem* 1948;40:1237-1242.
5. HJ, Philipp; CM, Conrad. Control of Elongation in Highly Stretched Cotton Tire Cord. *J. Appl. Phys.* 1945;16:32-40.
6. G, Raumann; JL, Brownlee. Tire Cord Application of High-Modulus Fibers Derived from Polyamide-Hydrazides. *J Macromol Sci A* 1973;A 7:281-293.
7. A, Manivannan; MS, Seehra. Identification and quantification of polymers in waste plastics using differential scanning calorimetry. *Abstr. Paper. Am. Chem. Soc.* 1997;214:20-FUEL.
8. P, Zhu; SY, Sui; B, Wang; K, Sun; G, Sun. A study of pyrolysis and pyrolysis products of flame-retardant cotton fabrics by DSC, TGA, and PY-GC-MS. *J. Anal. Appl. Pyrolysis* 2004;71:645-655.
9. PA, Eriksson; AC, Albertsson; K, Eriksson; JAE, Manson. Thermal oxidative stability of heat-stabilised polyamide 66 by differential scanning calorimetry. *J. Therm. Anal.* 1998;53:19-26.
10. S, Eve; M, Gomina; G, Orange, Euro Ceramics VIII: Effects of polyamide and polypropylene fibers on the setting and the mechanical properties of plaster, 264-268, 2531-2535.
11. S, Eve; M, Gomina; A, Gmouh; A, Samdi; R, Moussa; G, Orange. Microstructural and mechanical behaviour of polyamide fiber-reinforced plaster composites. *J. European Ceram. Soc.* 2002;22:2269-2275.
12. S, Eve; M, Gomina; J, Hamel; G, Orange, Investigation of the setting of polyamide fiber/latex-filled plaster composites. *J. European Ceram. Soc.* 2006;26:2541 - 2546.